

Analysis of a quenched lattice-QCD dressed-quark propagator

M.S. Bhagwat,¹ M.A. Pichowsky,¹ C.D. Roberts,² and P.C. Tandy¹

¹*Center for Nuclear Research, Department of Physics,
Kent State University, Kent, Ohio 44242 U.S.A.*

²*Physics Division, Argonne National Laboratory, Argonne, IL 60439-4843 U.S.A.*

(Dated: September 10, 2018)

Quenched lattice-QCD data on the dressed-quark Schwinger function can be correlated with dressed-gluon data via a rainbow gap equation so long as that equation's kernel possesses enhancement at infrared momenta above that exhibited by the gluon alone. The required enhancement can be ascribed to a dressing of the quark-gluon vertex. The solutions of the rainbow gap equation exhibit dynamical chiral symmetry breaking and are consistent with confinement. The gap equation and related, symmetry-preserving ladder Bethe-Salpeter equation yield estimates for chiral and physical pion observables that suggest these quantities are materially underestimated in the quenched theory: $|\langle\bar{q}q\rangle|$ by a factor of two and f_π by 30%.

PACS numbers: 12.38.Lg, 12.38.Gc, 12.38.Aw, 24.85.+p

I. INTRODUCTION

It is a longstanding prediction that the Schwinger functions which characterise the propagation of QCD's elementary excitations: gluons, ghosts and quarks, are strongly modified at infrared momentum scales, namely, spacelike momenta $k^2 \lesssim 2 \text{ GeV}^2$ [1, 2, 3]. Indeed, this property of asymptotically free theories was elucidated in Refs. [4, 5] and could be anticipated from studies of strong coupling QED [6]. Such momentum-dependent dressing is a fundamental feature of strong QCD that is observable in hadronic phenomena [7]. For example: it is the mechanism by which the current-quark mass evolves to assume the scale of a constituent-quark mass at infrared momenta, and thereby that dynamical chiral symmetry breaking (DCSB) is exhibited; and it may also provide an understanding of confinement, as we canvass in Sec. III D. These are keystones of hadron physics [8].

Numerical simulations of lattice-QCD provide direct access to QCD's Schwinger functions, and recent studies of the quenched theory yield dressed-gluon [9, 10, 11, 12] and -quark [13, 14] two-point functions ("propagators") that are in semi-quantitative agreement with Dyson-Schwinger equation (DSE) calculations [15, 16, 17, 18, 19, 20, 21]. However, these dressed-gluon and -quark propagators are not obviously consistent with each other in the following sense: use of the lattice dressed-gluon two-point function as the sole basis for the kernel of QCD's gap equation cannot yield the lattice dressed-quark propagator without a material infrared modification (enhancement) of the dressed-quark-gluon vertex [22, 23, 24]. Fortunately, just such behaviour can be understood to arise owing to multiplicative renormalisability of the gap equation [25, 26] and is observed in lattice estimates of this three-point function [27, 28, 29].

Herein we elucidate these points using a concrete model for the gap equation's kernel. Naturally, since the ultraviolet behaviour of this kernel is fixed by perturbative QCD and hence model-independent, our study will focus on and expose aspects of the infrared behaviour of

the Schwinger functions described above.

Furthermore, as indicated at the outset, DCSB is encoded in the chiral-limit behaviour of the dressed-quark propagator. However, contemporary lattice-QCD simulations are restricted to current-quark masses that are too large for unambiguous statements to be made about the magnitude of this effect. With a well-constrained model for the gap equation's kernel it is straightforward to calculate the dressed-quark propagator in the chiral limit. Hence our analysis will also provide an informed estimate of the chiral limit behaviour of the lattice results.

Finally, we consider two additional questions; namely, how do Schwinger functions obtained in simulations of quenched lattice-QCD differ from those in full QCD, and can that difference be used to estimate the effect of quenching on physical observables? Our model for the gap equation's kernel provides a foundation from which we believe these problems can fruitfully be addressed.

The article is organised as follows. In Sec. II we review the gap equation, the form of its solution and the nature of its kernel. Section III describes the construction of a model for the gap equation's kernel that correlates lattice results for the dressed-gluon and -quark two point functions, and explains aspects of the dressed-quark function obtained therewith. The kernel is exploited further in Sec. IV, wherein it provides the basis for calculating informed estimates of observable quantities in quenched-QCD. Section V is an epilogue.

II. GAP EQUATION

The renormalised dressed-quark propagator, $S(p)$, is the solution of the DSE

$$S^{-1}(p) = Z_2(\zeta, \Lambda) i \gamma \cdot p + Z_4(\zeta, \Lambda) m(\zeta) + \Sigma'(p, \Lambda), \quad (1)$$

wherein the dressed-quark self-energy is¹

$$\Sigma'(p, \Lambda) = Z_1(\zeta, \Lambda) \int_q^\Lambda g^2 D_{\mu\nu}(p-q) \frac{\lambda^i}{2} \gamma_\mu S(q) \Gamma_\nu^i(q, p). \quad (2)$$

Here $D_{\mu\nu}(k)$ is the renormalised dressed gluon propagator; $\Gamma_\nu^i(q, p)$ is the renormalised dressed quark-gluon vertex; and $Z_1(\zeta, \Lambda)$, $Z_2(\zeta, \Lambda)$ and $Z_4(\zeta, \Lambda)$ are, respectively, Lagrangian renormalisation constants for the quark-gluon vertex, quark wave function and current-quark mass.

In Eq. (2), $\int_q^\Lambda := \int^\Lambda d^4q / (2\pi)^4$ denotes a translationally invariant ultraviolet regularisation of the momentum space integral, with regularisation mass-scale Λ . In practice a Pauli-Villars scheme is used, in which an additional factor of $\Lambda^2 / (\Lambda^2 + (p-q)^2)$ is included with the gluon propagator. The resulting integral is finite $\forall \Lambda < \infty$, and develops a logarithmic divergence when the regularisation is removed; i.e., $\Lambda \rightarrow \infty$, which is the final stage of any calculation. We emphasise that it is only with a translationally invariant regularisation scheme that Ward-Takahashi identities can be preserved, something that is crucial to ensuring, e.g., axial-vector current conservation in the chiral limit.

The general form of the dressed-quark propagator is

$$S(p) = \frac{Z(p^2; \zeta^2)}{i\gamma \cdot p + M(p^2)} \quad (3)$$

where the Lorentz scalar functions $Z(p^2; \zeta^2)$ and $M(p^2)$ are respectively referred to as the quark wave function renormalisation and running quark mass (or dressed-quark mass-function). The renormalisation constants Z_2 and Z_4 are determined by solving the gap equation, Eq. (1), subject to the renormalisation condition that at some large spacelike ζ^2

$$S^{-1}(p) \Big|_{p^2=\zeta^2} = i\gamma \cdot p + m(\zeta), \quad (4)$$

where $m(\zeta)$ is the renormalised current-quark mass. The renormalised dressed-quark propagator is independent of the regularisation mass-scale, Λ . It depends on the renormalisation point, ζ , in a manner prescribed by the theory's dynamics. This dependence is expressed in the calculable ζ -dependence of the wave function renormalisation. The dressed-quark mass-function is independent of the regularisation mass-scale and of the renormalisation point. Once the renormalisation scheme has been faithfully applied the regularisation mass-scale may be removed to infinity.

Given the form of the dressed gluon propagator, $D_{\mu\nu}(p-q)$, and dressed quark-gluon vertex, $\Gamma_\mu^i(q, p)$, it is

straightforward to determine the corresponding dressed quark propagator using well-established numerical methods. A particularly important characteristic of the non-linear integral equation in Eq. (1) is that it yields a nonzero solution for $M(p^2)$ in the chiral limit [17, 30]:

$$Z_4(\zeta, \Lambda) m(\zeta) \equiv 0, \quad \Lambda \gg \zeta, \quad (5)$$

if, and only if, there is sufficient infrared support in the integrand. This is dynamical chiral symmetry breaking, which we discuss further in Sec. IV A. It is noteworthy that for finite ζ and $\Lambda \rightarrow \infty$, the left hand side (l.h.s.) of Eq. (5) is identically zero, by definition, because the mass term in QCD's Lagrangian density is renormalisation-point-independent. The condition specified in Eq. (5), on the other hand, effects the result that at the (perturbative) renormalisation point there is no mass-scale associated with explicit chiral symmetry breaking, which is the essence of the chiral limit.

As will now be plain, the kernel of the gap equation, Eq. (1), is formed from the product of the dressed-gluon propagator and dressed-quark-gluon vertex. The equation is therefore coupled to the DSEs satisfied by these functions. Those equations in turn involve other n -point functions and hence a tractable problem is only realised once a truncation scheme is specified. At least one non-perturbative, chiral symmetry preserving truncation exists [31, 32] and the first term in that scheme is the renormalisation-group-improved rainbow gap equation, wherein the self-energy, Eq. (2), assumes the form

$$\int_q^\Lambda \mathcal{G}(Q^2) D_{\mu\nu}^{\text{free}}(Q) \frac{\lambda^a}{2} \gamma_\mu S(q) \frac{\lambda^a}{2} \gamma_\nu, \quad (6)$$

where $Q = p - q$ and $D_{\mu\nu}^{\text{free}}(Q)$ is the Landau gauge free-gluon propagator.

In Eq. (6), $\mathcal{G}(Q^2)$ is an effective interaction, which expresses the combined effect of dressing both the gluon propagator and quark-gluon vertex consistent with the constraints imposed by, e.g., vector and axial-vector Ward-Takahashi identities. Asymptotic freedom entails

$$\mathcal{G}(Q^2) = 4\pi \alpha(Q^2), \quad Q^2 \gtrsim 2 \text{ GeV}^2; \quad (7)$$

viz., the effective interaction is proportional to the strong running coupling in the ultraviolet. However, its form is unknown for $Q^2 \lesssim 2 \text{ GeV}^2$. An explanation of many diverse hadron phenomena has been obtained by modelling this behaviour [7] but our goal is different. Hereinafter we explore the ramifications of employing the dressed-gluon propagator inferred from numerical simulations of lattice-QCD in building the effective interaction.

III. ANALYSING LATTICE DATA

A. Lattice gluon propagator

In Ref. [9] the Landau gauge dressed gluon propagator was computed using quenched lattice-QCD configu-

[1] We use a Euclidean metric wherewith the scalar product of two four vectors is $a \cdot b = \sum_{i=1}^4 a_i b_i$, and Hermitian Dirac- γ matrices that obey $\{\gamma_\mu, \gamma_\nu\} = 2\delta_{\mu\nu}$.

rations and the result was parametrised as:

$$D(k^2) = Z_g \left[\frac{A\Lambda_g^{2\alpha}}{(k^2 + \Lambda_g^2)^{1+\alpha}} + \frac{L(k^2, \Lambda_g)}{k^2 + \Lambda_g^2} \right], \quad (8)$$

with

$$\begin{aligned} A &= 9.8_{-0.9}^{+0.1}, & \Lambda_g &= 1.020 \pm 0.1 \pm 0.025 \text{ GeV}, \\ \alpha &= 2.2_{-0.2-0.3}^{+0.1+0.2}, & Z_g &= 2.01_{-0.05}^{+0.04}, \end{aligned} \quad (9)$$

where the first pair of errors are statistical and the second, when present, denote systematic errors associated with finite lattice spacing and volume. In the simulation the lattice spacing $a = 1/[1.885 \text{ GeV}]$. The numerator in the second term of Eq. (8) is

$$L(k^2, \Lambda_g) = \left(\frac{1}{2} \ln \left[(k^2 + \Lambda_g^2) \left(\frac{1}{k^2} + \frac{1}{\Lambda_g^2} \right) \right] \right)^{-d_D}, \quad (10)$$

with $d_D = [39 - 9\xi - 4N_f]/[2(33 - 2N_f)]$, an expression which ensures the parametrisation expresses the correct one-loop behaviour at ultraviolet momenta. In the quenched, Landau-gauge study, $N_f = 0$, $\xi = 0$, so

$$d_D = 13/22. \quad (11)$$

B. Effective quark-gluon vertex

We have noted that for $Q^2 \gtrsim 2 \text{ GeV}^2$ in Eq. (6)

$$\mathcal{G}(Q^2) = \frac{4\pi^2\gamma_m}{\ln(Q^2/\Lambda_{\text{QCD}}^2)}, \quad (12)$$

where $\gamma_m = 12/(33 - 2N_f)$ is the anomalous mass dimension. To proceed we therefore write

$$\frac{1}{Q^2} \mathcal{G}(Q^2) = D(Q^2) \Gamma_1(Q^2), \quad (13)$$

with $D(Q^2)$ given in Eq. (8) and

$$\Gamma_1(Q^2) = 4\pi^2\gamma_m \frac{1}{Z_g} \frac{[\frac{1}{2} \ln(\tau + Q^2/\Lambda_g^2)]^{d_D}}{[\ln(\tau + Q^2/\Lambda_{\text{QCD}}^2)]} v(Q^2), \quad (14)$$

where $\tau = e^2 - 1 > 1$ is an infrared cutoff. Equation (13) factorises the effective interaction into a contribution from the lattice dressed-gluon propagator multiplied by a contribution from the vertex, which we shall subsequently determine phenomenologically.

We remark that the renormalisation-group-improved rainbow truncation retains only that single element of the dressed-quark-gluon vertex which is ultraviolet divergent at one-loop level and this explains the simple form of Eq. (14). Systematic analyses of corrections to the rainbow truncation show Γ_1 to be the dominant amplitude of the dressed vertex: the remaining amplitudes do not significantly affect observables [32]. In proceeding

phenomenologically solely with Γ_1 , we force $v(Q^2)$ to assume the role of the omitted amplitudes to the maximum extent possible.

In Eq. (14), so long as $v(Q^2) \simeq 1$ for $Q^2 \gtrsim 2 \text{ GeV}^2$, Eq. (12) is satisfied and consequently the rainbow gap equation preserves the renormalisation group flow of QCD at one-loop. We therefore consider a simple *Ansatz* with this property:

$$v(Q^2) = \frac{a_v(m) + Q^2/\Lambda_g^2}{b + Q^2/\Lambda_g^2}, \quad (15)$$

where

$$a_v(m) = \frac{a_1}{1 + a_2 [m(\zeta)/\Lambda_g] + a_3 [m(\zeta)/\Lambda_g]^2} \quad (16)$$

and $a_{1,2,3}$ and b are dimensionless parameters, which are fitted by requiring that the gap equation yield a solution for the dressed-quark propagator that agrees well pointwise with the results obtained in numerical simulations of quenched lattice-QCD [13, 14]. It is important to note that a good fit to lattice data is impossible unless $a_v(m)$ depends on the current-quark mass. While more complicated forms are clearly possible, the *Ansatz* of Eq. (16) is adequate.

C. Fit to lattice results

Now, to be explicit, the parameters in Eqs. (15), (16) were determined by the following procedure. The rainbow gap equation; viz., Eq. (1) simplified via Eq. (6), was solved using the effective interaction specified by Eqs. (13)–(16), with $D(Q^2)$ exactly as given in Eq. (8).

The ultraviolet behaviour of the mass function, $M(p^2)$, is determined by perturbative QCD and is therefore model independent. Hence the current-quark mass, $m(\zeta)$, was fixed by requiring agreement between the DSE and lattice results for $M(p^2)$ on $p^2 \gtrsim 1 \text{ GeV}^2$. We selected three lattice data sets from Ref. [14] and, for consistency with Refs. [17, 18], used a renormalisation point $\zeta = 19 \text{ GeV}$, which is well into the perturbative domain. This gave

$$\frac{a m_{\text{lattice}}}{m(\zeta)(\text{GeV})} \left| \begin{array}{ccc} 0.018 & 0.036 & 0.072 \\ 0.030 & 0.055 & 0.110 \end{array} \right. . \quad (17)$$

The dimensionless parameters $a_{1,2,3}$ and b were subsequently determined in a simultaneous least-squares fit of DSE solutions for $M(p^2)$ at these current-quark masses to all the lattice data. This necessarily required the gap equation to be solved repeatedly. Nevertheless, the fit required only hours on a modern workstation, and yielded:

$$\frac{a_1}{1.5} \left| \frac{a_2}{7.35} \right| \left| \frac{a_3}{63.0} \right| \left\| \frac{b}{0.005} \right. . \quad (18)$$

These parameters completely determine the “best-fit effective-interaction” and hence our lattice-constrained model for the gap equation’s kernel.

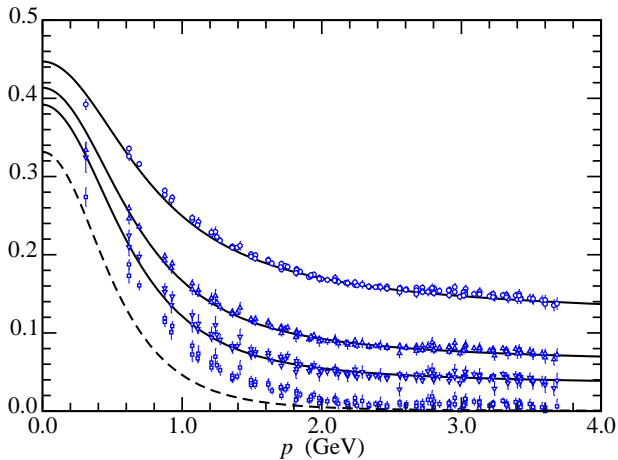


FIG. 1: Data, upper three sets: lattice results for $M(p^2)$ in GeV at am values in Eq. (17); lower points (boxes): linear extrapolation of lattice results [14] to $am = 0$. Solid curves: best-fit-interaction gap equation solutions for $M(p^2)$ obtained using the current-quark masses in Eq. (17); dashed-curve: gap equation's solution in the chiral limit, Eq. (5).

We emphasise that because the comparison is with simulations of quenched lattice-QCD, we used $N_f = 0$ throughout and [27, 28, 29, 33]

$$\Lambda_{\text{qu-QCD}} = 0.234 \text{ GeV}. \quad (19)$$

The strength of the running strong coupling is underestimated in simulations of quenched lattice-QCD [34]. (NB. Halving or doubling $\Lambda_{\text{qu-QCD}}$ has no material quantitative impact on the results reported in Sec. IV, nor does it qualitatively affect our conclusions.)

1. Fidelity and quiddity of the procedure

In Fig. 1 we compare DSE solutions for $M(p^2)$, obtained using the optimised effective interaction, with lattice results. In addition, we depict the DSE solution for $M(p^2)$ calculated in the chiral limit along with the linear extrapolation of the lattice data to $am = 0$, as described in Ref. [13]. It is apparent that the lattice-gluon and lattice-quark propagators can be correlated via the renormalisation-group-improved gap equation. That was achieved via $v(Q^2)$ in Eq. (15), and the required form is depicted in Fig. 2. Plainly, consistency between the propagators via this gap equation requires an infrared enhancement of the vertex, as anticipated in Refs. [22, 23, 25, 26]. Our inferred form is in semi-quantitative agreement with the result of recent, exploratory lattice-QCD simulations of the dressed-quark-gluon vertex [27, 28, 29].

Dynamical chiral symmetry breaking is another important feature evident in Fig. 1; viz., the existence of a $M(p^2) \neq 0$ solution of the gap equation in the chiral limit. We deduce that DCSB is manifest in quenched-QCD and,

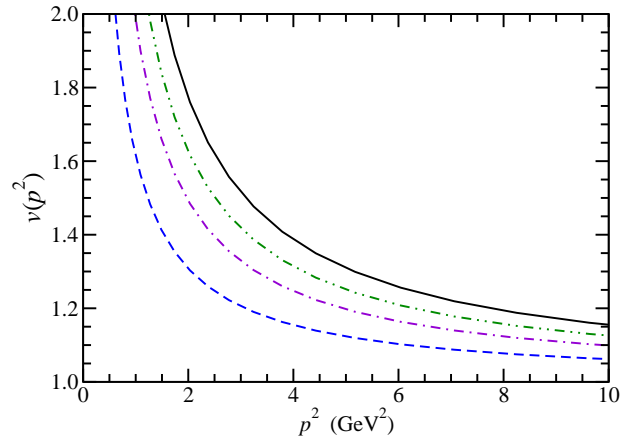


FIG. 2: Dimensionless vertex dressing factor: $v(Q^2)$, defined via Eqs. (15), (16), (18), obtained in the chiral limit (*solid curve*) and with the current-quark masses in Eq. (17). $v(Q^2)$ is finite at $Q^2 = 0$ and decreases with increasing $m(\zeta)$.

in the following, quantify the magnitude of that effect. It should be observed that a linear extrapolation to $am = 0$ of the lattice data obtained with nonzero current-quark masses overestimates the mass function calculated directly as the solution of the gap equation.

Figure 3 focuses on the lattice simulations for the intermediate value of the current-quark mass; namely, $am = 0.036$, and compares lattice output for both $M(p^2)$ and the quark wave function renormalisation, $Z(p^2)$, with our results. We emphasise that the form of $Z(p^2)$ was not used in fitting $v(Q^2)$. Hence the pointwise agreement between the gap equation's solution and the lattice result indicates that our simple expression for the effective interaction captures the dominant dynamical content and, in particular, that omitting the subdominant amplitudes in the dressed-quark-gluon vertex is not a serious flaw in this study.

D. Spectral properties

In a quantum field theory defined by a Euclidean measure [35] the Osterwalder-Schrader axioms [36, 37] are five conditions which any moment of this measure (n -point Schwinger function) must satisfy if it is to have an analytic continuation to Minkowski space and hence an association with observable quantities. One of these is ‘‘OS3’’: the axiom of *reflection positivity*, which is violated if the Schwinger function's Fourier transform to configuration space is not positive definite. The space of observable asymptotic states is spanned by eigenvectors of the theory's infrared Hamiltonian and no Schwinger function that breaches OS3 has a correspondent in this space. Consequently, the violation of OS3 is a sufficient condition for confinement.

This connection has long been of interest [38, 39], and is discussed at length in Refs. [40, 41, 42], and reviewed

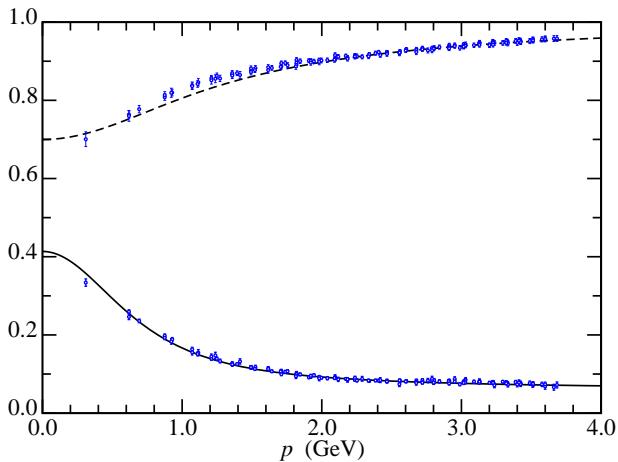


FIG. 3: Data, quenched lattice-QCD results for $M(p^2)$ and $Z(p^2)$ obtained with $am = 0.036$ [14]; dashed curve, $Z(p^2)$, and solid curve, $M(p^2)$ calculated from the gap equation with our optimised effective interaction and $m(\zeta) = 55$ MeV. (NB. $Z(p^2)$ is dimensionless and $M(p^2)$ is measured in GeV.)

in Sec. 6.2 of Ref. [1], Sec. 2.2 of Ref. [2] and Sec. 2.4 of Ref. [3]. It suggests and admits a practical test [22] that has been exploited in Refs. [20, 22, 23, 43, 44, 45, 46, 47, 48, 49] and which for the quark 2-point function is based on the behaviour of

$$\begin{aligned} \Delta_S(T) &= \int d^3x \int \frac{d^4p}{(2\pi)^4} e^{ip \cdot x} \sigma_S(p^2) \quad (20) \\ &= \frac{1}{\pi} \int_0^\infty d\varepsilon \cos(\varepsilon T) \sigma_S(\varepsilon^2), \quad (21) \end{aligned}$$

where σ_S is the Dirac-scalar projection of the dressed-quark propagator. For a noninteracting fermion with mass μ ,

$$\Delta_S^{\text{free}}(T) = \frac{1}{\pi} \int_0^\infty d\varepsilon \cos(\varepsilon T) \frac{\mu}{\varepsilon^2 + \mu^2} = \frac{1}{2} e^{-\mu T}. \quad (22)$$

The r.h.s. is positive definite. It is also plainly related via analytic continuation ($T \rightarrow it$) to the free-particle solution of the Minkowski space Dirac equation. The existence of an associated asymptotic state is indubitable.

If instead one encountered a theory in which [41, 42, 49]

$$\sigma_S(p^2) = \frac{\mu}{2} \left[\frac{1}{p^2 + \mu^2 - i\rho^2} + \frac{1}{p^2 + \mu^2 + i\rho^2} \right], \quad (23)$$

a function with poles at $p^2 + \sigma^2 \exp(\pm i\theta) = 0$, where

$$\sigma^4 = \mu^4 + \rho^4, \quad \tan \theta = \rho^2 / \mu^2, \quad (24)$$

then

$$\Delta_S(T) = \frac{\mu}{2\sigma} e^{-\sigma T \cos \frac{\theta}{2}} \cos \left(\sigma T \sin \frac{\theta}{2} + \frac{\theta}{2} \right). \quad (25)$$

This Fourier transform has infinitely many, regularly spaced zeros and hence OS3 is violated. Thus the fermion

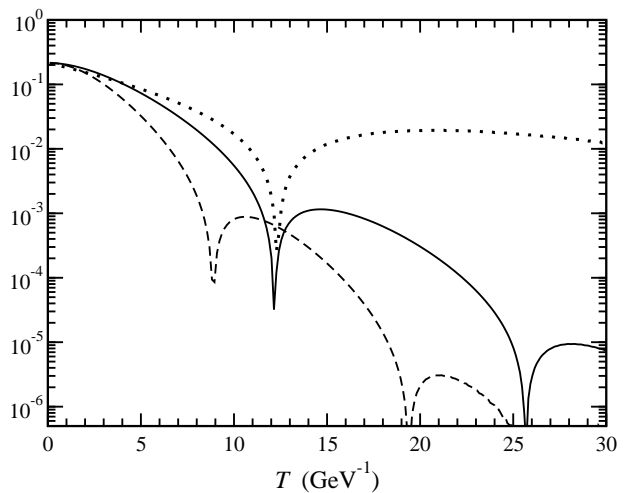


FIG. 4: $|\Delta_S(T)|$ obtained from: the chiral limit gap equation solution calculated using our lattice-constrained kernel, solid curve; Eq. (23) with $\sigma = 0.13$ GeV, $\theta = \pi/2.46$, dotted curve; the model of Ref. [18], dashed curve.

described by this Schwinger function has no correspondent in the space of observable asymptotic states.

It is readily apparent that Eq. (23) evolves to a free particle propagator when $\rho \rightarrow 0$. This limit is expressed in Eq. (25) via $\theta \rightarrow 0$, $\sigma \rightarrow \mu$, wherewith Eq. (22) is recovered; a result that is tied to the feature that the first zero of $\Delta_S(T)$ in Eq. (25) occurs at

$$z_1 = \frac{\pi - \theta}{2\sigma} \csc \frac{\theta}{2} \quad (26)$$

and hence $z_1 \rightarrow \infty$ for $\rho \rightarrow 0$ [43, 44].

We calculated $\Delta_S(T)$ using the gap equation solutions discussed above and the form of $|\Delta_S(T)|$ obtained with the chiral limit solution is depicted in Fig. 4. The violation of OS3 is manifest in the appearance of cusps: $\ln |\Delta_S(T)|$ is negative and infinite in magnitude at zeros of $\Delta_S(T)$. The differences evident in a comparison with the result obtained from Eq. (25) indicate that the singularity structure of the dressed-quark 2-point Schwinger function obtained from the lattice-constrained kernel is more complicated than just a single pair of complex conjugate poles. However, the similarities suggest that this picture may serve well as an idealisation [49]. (NB. Qualitatively identical results are obtained using $\sigma_V(p^2)$, the Dirac-vector projection of the dressed-quark propagator, instead of $\sigma_S(p^2)$.)

Figure 4 also portrays the result obtained with the effective interaction proposed in Ref. [18] and used efficaciously in studies of meson properties [7]. Significantly, the first zero appears at a smaller value of T in this case. Using the model of Eq. (23) as a guide, that shift indicates a larger value of σ . This sits well with the fact that the mass-scale generated dynamically by the interaction of Ref. [18] is larger than that produced by the interaction used herein, which is only required to correlate

quenched lattice data for the gluon and quark two-point functions.

From the results and analysis reported in this subsection, we deduce that light-quarks do not appear in the space of observable asymptotic states associated with quenched-QCD; an outcome anticipated in Ref. [26].

IV. CHIRAL AND PHYSICAL PION OBSERVABLES

A. Chiral limit

The scale of DCSB is measured by the value of the renormalisation-point dependent vacuum quark condensate, which is obtained directly from the chiral limit dressed-quark propagator [17, 30]:

$$-\langle \bar{q}q \rangle_{\zeta}^0 = \lim_{\Lambda \rightarrow \infty} Z_4(\zeta, \Lambda) N_c \operatorname{tr} \int_q^{\Lambda} S_0(q), \quad (27)$$

where “tr” denotes a trace only over Dirac indices and the index “0” labels a quantity calculated in the chiral limit, Eq. (5). In Eq. (27) the gauge parameter dependence of the renormalisation constant Z_4 is precisely that required to ensure the vacuum quark condensate is gauge independent. This constant is fixed by the renormalisation condition, Eq. (4), which entails

$$Z_4(\zeta, \Lambda) = -\frac{1}{m(\zeta)} \frac{1}{4} \operatorname{tr} \Sigma'(\zeta, \Lambda) \quad (28)$$

wherein the right hand side is well-defined in the chiral limit [17]. (It may also be determined by studying the fully amputated pseudoscalar-quark-antiquark 3-point function [30].) A straightforward calculation using our chiral limit result; i.e, the propagator corresponding to the dashed-curve in Fig. 1, yields

$$-\langle \bar{q}q \rangle_{\zeta=19 \text{ GeV}}^0 = (0.22 \text{ GeV})^3. \quad (29)$$

To evolve the condensate to a “typical hadronic scale,” e.g., $\zeta = 1 \text{ GeV}$, one may use [50]

$$\langle \bar{q}q \rangle_{\zeta'}^0 = Z_4(\zeta', \zeta) Z_2^{-1}(\zeta', \zeta) \langle \bar{q}q \rangle_{\zeta}^0 =: Z_m(\zeta', \zeta) \langle \bar{q}q \rangle_{\zeta}^0, \quad (30)$$

where Z_m is the gauge invariant mass renormalisation constant. Contemporary phenomenological approaches employ the one-loop expression for Z_m and following this expedient we obtain, practically as a matter of definition,

$$\begin{aligned} -\langle \bar{q}q \rangle_{1 \text{ GeV}}^0 &= \left(\frac{\ln[1/\Lambda_{\text{qu-QCD}}]}{\ln[19/\Lambda_{\text{qu-QCD}}]} \right)^{\gamma_m} (-\langle \bar{q}q \rangle_{19 \text{ GeV}}^0) \\ &= (0.19 \text{ GeV})^2, \end{aligned} \quad (31)$$

which may be compared with a best-fit phenomenological value [51]: $(0.24 \pm 0.01 \text{ GeV})^3$. It is notable that DSE models which efficaciously describe light-meson physics; e.g., Refs. [17, 18], give $\langle \bar{q}q \rangle_{1 \text{ GeV}}^0 = -(0.24 \text{ GeV})^3$.

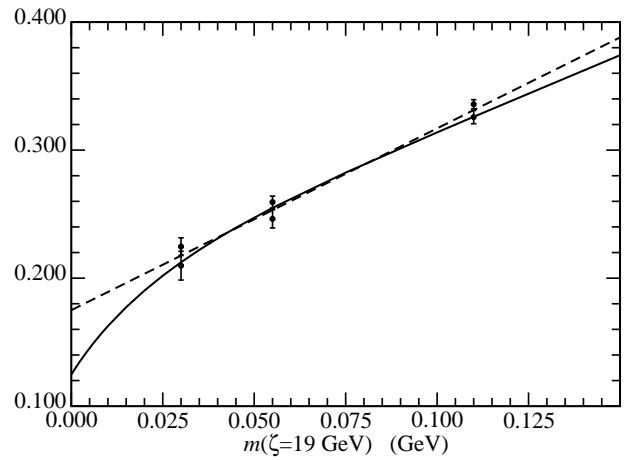


FIG. 5: $M(p_{\text{IR}}^2 = 0.38 \text{ GeV}^2)$, in GeV, as a function of the current-quark mass. Solid curve, our result; circles, lattice data for am in Eq. (amvalues) [14]; dashed-line, linear fit to the lattice data, Eq. (32).

Our gap equation assisted estimate therefore indicates that the chiral condensate in quenched-QCD is a factor of two smaller than that which is obtained from analyses of strong interaction observables. These results are in quantitative agreement with Ref. [26].

A fit to the linear extrapolation of the lattice data; viz., to the boxes in Fig. 1, gives a significantly larger value [14]: $-\langle \bar{q}q \rangle_{1 \text{ GeV}}^0 = (0.270 \pm 0.027 \text{ GeV})^3$. However, the error is purely statistical. The systematic error, to which the linear extrapolation must contribute, was not estimated. That may be important given the discrepancy, conspicuous in Fig. 1, between our direct evaluation of the chiral limit mass function and the linear extrapolation of the lattice data to $am = 0$: the linear extrapolation lies well above the result of our chiral limit calculation.

This point may be illustrated further. In Fig. 5 we plot $M(p^2 = p_{\text{IR}}^2)$, where $p_{\text{IR}} = 0.62 \text{ GeV}$, as a function of the current-quark mass (*solid curve*). This value of the argument was chosen because it is the smallest p^2 for which there are two lattice results for $M(p^2)$ at each current-quark mass in Eq. (17). Those results are also plotted in the figure. It is evident that on the domain of current-quark masses directly accessible in lattice simulations, the lattice and DSE results lie on the same linear trajectory, of which

$$M(p_{\text{IR}}^2 = 0.38 \text{ GeV}^2, m(\zeta)) = 0.18 + 1.42 m(\zeta) \quad (32)$$

provides an adequate interpolation. However, as apparent in the figure, this fit on $am \in [0.018, 0.072]$ provides a poor extrapolation to $m(\zeta) = 0$, giving a result 40% too large.

In Fig. 6 we repeat this procedure, focusing solely on our value of $M(p^2 = 0)$ because directly calculated lattice data are unavailable at this extreme infrared point and published estimates obtained by extrapolating functions fitted to the lattice- p^2 -dependence are inconsistent

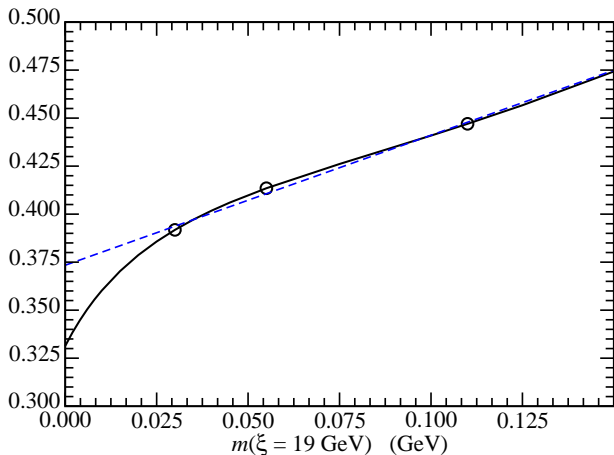


FIG. 6: Solid curve, calculated $M(p^2 = 0)$, in GeV, as a function of the current-quark mass $m(\zeta)$. The circles mark the current-quark masses in Eq. (17). Dashed-line, linear interpolation of our result for $M(p^2 = 0)$ on this mass domain.

[13]. The pattern observed in Fig. 5 is again visible. On the domain of current-quark masses for which lattice data are available, the mass-dependence of $M(p^2)$ is well-approximated by a straight line; namely,

$$M(p^2 = 0, m(\zeta)) = 0.37 + 0.68 m(\zeta), \quad (33)$$

but the value of $M(0)$ determined via extrapolation to $m(\zeta) = 0$ is 14% too large.

In all cases our calculated result possesses significant curvature. At fixed p^2 , $M(p^2, m(\zeta))$ is a monotonically increasing function of $m(\zeta)$ but, while it is concave-down for $m(\zeta) \lesssim 0.1$ GeV, it inflects thereafter to become concave-up. In addition, at fixed $m(\zeta)$, $M(p^2)$ is a monotonically decreasing function of p^2 . It follows that a linear extrapolation determined by data on $am \in [0.018, 0.072]$ will necessarily overestimate $M(p^2)$ at all positive values of p^2 . The figures illustrate that the error owing to extrapolation increases with increasing p^2 and hence a significant overestimate can be anticipated on the domain in which the condensate was inferred from lattice data.

It is straightforward to understand the behaviour evident in Figs. 5, 6 qualitatively. The existence of DCSB means that in the neighbourhood of the chiral limit a mass-scale other than the current-quark mass determines the magnitude of $M(p^2)$. As the current-quark mass increases from zero, its magnitude will come to affect that of the mass function. The gap equation is a nonlinear integral equation and hence this evolution of the mass-dependence of $M(p^2)$ will in general be nonlinear. Only at very large values of the current-quark mass will this scale dominate the behaviour of the mass function, as seen in studies of heavy-quark systems [52], and the evolution become linear.

B. Pion properties

The renormalised homogeneous Bethe-Salpeter equation (BSE) for the isovector-pseudoscalar channel; i.e., the pion, is

$$[\Gamma_\pi^j(k; P)]_{tu} = \int_q^\Lambda [\chi_\pi^j(q; P)]_{sr} K_{tu}^{rs}(q, k; P), \quad (34)$$

where k is the relative momentum of the quark-antiquark pair, P is their total momentum; and

$$\chi_\pi^j(q; P) = S(q_+) \Gamma_\pi^j(q; P) S(q_-), \quad (35)$$

with $\Gamma_\pi^j(k; P)$ the pion's Bethe-Salpeter amplitude, which has the general form

$$\Gamma_\pi^j(k; P) = \tau^j \gamma_5 \left[i E_\pi(k; P) + \gamma \cdot P F_\pi(k; P) + \gamma \cdot k k \cdot P G_\pi(k; P) + \sigma_{\mu\nu} k_\mu P_\nu H_\pi(k; P) \right]. \quad (36)$$

In Eq. (34), $K(q, k; P)$ is the fully-amputated quark-antiquark scattering kernel, and the axial-vector Ward-Takahashi identity requires that this kernel and that of the gap equation must be intimately related. The consequences of this are elucidated in Refs. [31, 32] and in the present case they entail

$$K_{tu}^{rs}(q, k; P) = -\mathcal{G}((k - q)^2) \times D_{\mu\nu}^{\text{free}}(q - k) \left[\frac{\lambda^a}{2} \gamma_\mu \right]_{ts} \left[\frac{\lambda^a}{2} \gamma_\nu \right]_{ru}, \quad (37)$$

which provides the renormalisation-group-improved ladder-truncation of the BSE. The efficacy of combining the renormalisation-group-improved rainbow-DSE and ladder-BSE truncations is exhibited in Ref. [7]. In particular, it guarantees that in the chiral limit the pion is both a Goldstone mode and a bound state of a strongly dressed-quark and -antiquark, and ensures consistency with chiral low energy theorems [53, 54].

All the elements involved in building the kernel of the pion's BSE were determined in the last section and hence one can solve for the pion's mass and Bethe-Salpeter amplitude. To complete this exercise practically we consider

$$[1 - \ell(P^2)] [\Gamma_5^j(k; P)]_{tu} = \int_q^\Lambda [\chi_5^j(q; P)]_{sr} K_{tu}^{rs}(q, k; P). \quad (38)$$

This equation has a solution for arbitrary P^2 and solving it one obtains a trajectory $\ell(P^2)$ whose first zero coincides with the bound state's mass, at which point $\Gamma_5^j(k; P)$ is the true bound state amplitude. In general, solving for $\ell(P^2)$ in the physical domain: $P^2 < 0$, requires that the integrand be evaluated at complex values of its argument. However, as $m_\pi^2 \ll M^2(0)$; i.e., the magnitude of the zero is much smaller than the characteristic dynamically-generated scale in this problem, we

	Calc. (quenched)	Experiment
m_π	0.1385	0.1385
f_π	0.066	0.0924
f_π^0	0.063	

TABLE I: Pion-related observables calculated using our lattice-constrained effective interaction. $m(\zeta = 19 \text{ GeV}) = 3.3 \text{ MeV}$ was chosen to give $m_\pi = 0.1395 \text{ GeV}$. The index “0” indicates a quantity obtained in the chiral limit.

avoid complex arguments by adopting the simple expedient of calculating $\ell(P^2 > 0)$ and extrapolating to locate its timelike zero. The Bethe-Salpeter amplitude is identified with the $P^2 = 0$ solution. Naturally, this expedient yields the exact solution in the chiral limit; and in cases where a comparison with the exact solution has been made for realistic, nonzero light-quark masses, the error is negligible [55], as we shall subsequently illustrate.

Once its mass and bound state amplitude are known, it is straightforward to calculate the pion’s leptonic decay constant [30]:

$$f_\pi \delta^{ij} 2 P_\mu = Z_2 \text{tr} \int_q^\Lambda \tau^i \gamma_5 \gamma_\mu \chi_\pi^j(q; P). \quad (39)$$

In this expression, the factor of Z_2 is crucial: it ensures the result is gauge invariant, and cutoff and renormalisation-point independent. (The Bethe-Salpeter amplitude is normalised canonically [56].)

Table I lists values of pion observables calculated using the effective interaction obtained in Sec. III C by fitting the quenched-QCD lattice data. (The nonzero current-quark mass in the table corresponds to a one-loop evolved value of $m(1 \text{ GeV}) = 5.0 \text{ MeV}$.) To aid with the consideration of these results we note that unquenched chiral-limit DSE calculations that accurately describe hadron observables give [18] $f_\pi^0 = 0.090 \text{ GeV}$. We infer from these results that the pion decay constant in quenched lattice-QCD is underestimated by 30%. Quantitatively equivalent results were found in Ref. [26].

The rainbow-ladder truncation of the gap and Bethe-Salpeter equations is chiral symmetry preserving: without fine-tuning it properly represents the consequences of chiral symmetry and its dynamical breaking. The truncation expresses the model-independent mass formula for flavour-nonsinglet pseudoscalar mesons [30] a corollary of which, at small current-quark masses, is the Gell–Mann–Oakes–Renner relation:

$$(f_\pi^0)^2 m_\pi^2 = -2 m(\zeta) \langle \bar{q}q \rangle_\zeta^0 + O(m^2(\zeta)). \quad (40)$$

Inserting our calculated values on the l.h.s. and r.h.s. of Eq. (40), we have

$$(0.093 \text{ GeV})^4 \text{ cf. } (0.091 \text{ GeV})^4; \quad (41)$$

viz, the same accuracy seen in exemplary coupled DSE-BSE calculations; e.g., Ref. [17]. This establishes the fidelity of our expedient for solving the BSE.

V. SUMMARY

We studied quenched-QCD using a rainbow-ladder truncation of the Dyson-Schwinger equations (DSEs) and demonstrated that existing results from lattice simulations of quenched-QCD for the dressed-gluon and -quark Schwinger functions can be correlated via a gap equation that employs a renormalisation-group-improved model interaction. As usual, the ultraviolet behaviour of this effective interaction is fully determined by perturbative QCD. For the infrared behaviour we employed an *Ansatz* whose parameters were fixed in a least squares fit of the gap equation’s solutions to lattice data on the dressed-quark mass function, $M(p^2)$, at available current-quark masses. With our best-fit parameters the mass functions calculated from the gap equation were indistinguishable from the lattice results. The gap equation simultaneously yields the dressed-quark renormalisation function, $Z(p^2)$, and, without tuning, our results agreed with those obtained in the lattice simulations.

To correlate the lattice’s dressed-gluon and -quark Schwinger functions it was necessary for the gap equation’s kernel to exhibit infrared enhancement over and above that observed in the gluon function alone. We attributed that to an infrared enhancement of the dressed-quark-gluon vertex. The magnitude of the vertex modification necessary to achieve the correlation is semi-quantitatively consistent with that observed in quenched lattice-QCD estimates of this three-point function.

With a well-defined effective interaction, the gap equation provides a solution for the dressed-quark Schwinger function at arbitrarily small current-quark masses and, in particular, in the chiral limit: no extrapolation is involved. A kernel that accurately describes dressed-quark lattice data at small current-quark masses may therefore be used as a tool with which to estimate the chiral limit behaviour of the lattice Schwinger function. Our view is that this method is a more reliable predictor than a linear extrapolation of lattice data to the chiral limit. Even failing to accept this perspective, the material difference between results obtained via the lattice-constrained gap equation and those found by linear extrapolation of the lattice data must be cause for concern in employing the latter.

In addition, from a well-defined gap equation it is straightforward to construct symmetry-preserving Bethe-Salpeter equations whose bound state solutions describe mesons. We illustrated this via the pion, and calculated its mass and decay constants in our DSE model of the quenched theory.

Finally, assuming that existing lattice-QCD data are not afflicted by large systematic errors associated with finite volume or lattice spacing, we infer from our analysis that quenched QCD exhibits dynamical chiral symmetry breaking and dressed-quark two-point functions that violate reflection positivity but that chiral and physical pion observables are significantly smaller in the quenched theory than in full QCD.

Acknowledgments

We thank P.O. Bowman for the lattice data, and acknowledge valuable interactions with P. Maris, R. Alkofer and C. Fischer. CDR is grateful for support from the Special Research Centre for the Subatomic Structure of Matter at the University of Adelaide, Australia, and the

hospitality of its staff during a visit in which some of this work was completed. This work was supported by: the Department of Energy, Nuclear Physics Division, under contract no. W-31-109-ENG-38; the National Science Foundation under contract nos. PHY-0071361 and INT-0129236; and benefited from the resources of the National Energy Research Scientific Computing Center.

-
- [1] C. D. Roberts and A. G. Williams, *Prog. Part. Nucl. Phys.* **33**, 477 (1994).
- [2] C. D. Roberts and S. M. Schmidt, *Prog. Part. Nucl. Phys.* **45**, S1 (2000).
- [3] R. Alkofer and L. von Smekal, *Phys. Rept.* **353**, 281 (2001).
- [4] K. D. Lane, *Phys. Rev. D* **10**, 2605 (1974).
- [5] H. D. Politzer, *Nucl. Phys.* **B117**, 397 (1976).
- [6] K. Johnson, M. Baker, and R. Willey, *Phys. Rev.* **136**, B1111 (1964).
- [7] P. Maris and C. D. Roberts (2003), *nucl-th/0301049*.
- [8] S. Capstick et al. (2000), “Key issues in hadronic physics,” *hep-ph/0012238*.
- [9] D. B. Leinweber, J. I. Skullerud, A. G. Williams, and C. Parrinello (UKQCD), *Phys. Rev. D* **60**, 094507 (1999).
- [10] C. Alexandrou, P. De Forcrand, and E. Follana, *Phys. Rev. D* **65**, 117502 (2002), and references therein.
- [11] P. O. Bowman, U. M. Heller, D. B. Leinweber, and A. G. Williams, *Phys. Rev. D* **66**, 074505 (2002), and references therein.
- [12] J. C. R. Bloch, A. Cucchieri, K. Langfeld, and T. Mendes (2002), “Running coupling constant and propagators in SU(2) Landau gauge,” *hep-lat/0209040*.
- [13] P. O. Bowman, U. M. Heller, and A. G. Williams, *Phys. Rev. D* **66**, 014505 (2002).
- [14] P. O. Bowman, U. M. Heller, D. B. Leinweber, and A. G. Williams (2002), “Modelling the quark propagator,” *hep-lat/0209129*.
- [15] L. von Smekal, A. Hauck, and R. Alkofer, *Ann. Phys.* **267**, 1 (1998).
- [16] D. Atkinson and J. C. R. Bloch, *Mod. Phys. Lett.* **A13**, 1055 (1998).
- [17] P. Maris and C. D. Roberts, *Phys. Rev. C* **56**, 3369 (1997).
- [18] P. Maris and P. C. Tandy, *Phys. Rev. C* **60**, 055214 (1999).
- [19] P. C. Tandy (2003), “Covariant QCD modeling of light meson physics,” *nucl-th/0301040*.
- [20] C. S. Fischer and R. Alkofer (2003), *hep-ph/0301094*.
- [21] D. Zwanziger (2003), “Non-perturbative Faddeev-Popov formula and infrared limit of QCD,” *hep-ph/0303028*.
- [22] F. T. Hawes, C. D. Roberts, and A. G. Williams, *Phys. Rev. D* **49**, 4683 (1994).
- [23] F. T. Hawes, P. Maris, and C. D. Roberts, *Phys. Lett.* **B440**, 353 (1998).
- [24] J. Papavassiliou and J. M. Cornwall, *Phys. Rev. D* **44**, 1285 (1991).
- [25] J. C. R. Bloch, *Phys. Rev. D* **66**, 034032 (2002).
- [26] P. Maris, A. Raya, C. D. Roberts, and S. M. Schmidt (2002), “Facets of confinement and dynamical chiral symmetry breaking,” *nucl-th/0208071*.
- [27] J. Skullerud and A. Kızılersü, *JHEP* **09**, 013 (2002).
- [28] J. Skullerud, P. Bowman, and A. Kızılersü (2002), “The nonperturbative quark gluon vertex,” *hep-lat/0212011*.
- [29] J. I. Skullerud, P. O. Bowman, A. Kızılersü, D. B. Leinweber, and A. G. Williams (2003), “Nonperturbative structure of the quark gluon vertex,” *hep-ph/0303176*.
- [30] P. Maris, C. D. Roberts, and P. C. Tandy, *Phys. Lett.* **B420**, 267 (1998).
- [31] A. Bender, C. D. Roberts, and L. Von Smekal, *Phys. Lett.* **B380**, 7 (1996).
- [32] A. Bender, W. Detmold, C. D. Roberts, and A. W. Thomas, *Phys. Rev. C* **65**, 065203 (2002).
- [33] A. X. El-Khadra, G. Hockney, A. S. Kronfeld, and P. B. Mackenzie, *Phys. Rev. Lett.* **69**, 729 (1992).
- [34] S. Aoki et al., *Phys. Rev. Lett.* **74**, 22 (1995).
- [35] J. Glimm and A. Jaffe (1981), *Quantum Physics. A Functional Point of View* (Springer-Verlag, New York).
- [36] K. Osterwalder and R. Schrader, *Commun. Math. Phys.* **31**, 83 (1973).
- [37] K. Osterwalder and R. Schrader, *Commun. Math. Phys.* **42**, 281 (1975).
- [38] J. M. Cornwall, *Phys. Rev. D* **22**, 1452 (1980), and references therein and thereto.
- [39] H. J. Munczek and A. M. Nemirovsky, *Phys. Rev. D* **28**, 181 (1983), and references therein and thereto.
- [40] G. Krein, C. D. Roberts, and A. G. Williams, *Int. J. Mod. Phys.* **A7**, 5607 (1992).
- [41] U. Habel, R. Konning, H. G. Reusch, M. Stingl, and S. Wigard, *Z. Phys.* **A336**, 435 (1990).
- [42] M. Stingl, *Z. Phys.* **A353**, 423 (1996).
- [43] A. Bender, D. Blaschke, Y. Kalinovsky, and C. D. Roberts, *Phys. Rev. Lett.* **77**, 3724 (1996).
- [44] A. Bender, G. I. Poulis, C. D. Roberts, S. M. Schmidt, and A. W. Thomas, *Phys. Lett.* **B431**, 263 (1998).
- [45] A. Bender and R. Alkofer, *Phys. Rev. D* **53**, 446 (1996).
- [46] P. Maris, *Phys. Rev. D* **52**, 6087 (1995).
- [47] D. Gomez Dumm and N. N. Scoccola, *Phys. Rev. D* **65**, 074021 (2002).
- [48] V. Sauli, *JHEP* **02**, 001 (2003).
- [49] M. Bhagwat, M. A. Pichowsky, and P. C. Tandy, *Phys. Rev. D* **67**, 054019 (2003).
- [50] K. Langfeld, H. Markum, R. Pullirsch, C. D. Roberts, and S. M. Schmidt (2003), “Concerning the quark condensate,” *nucl-th/0301024*.
- [51] D. B. Leinweber, *Annals Phys.* **254**, 328 (1997).
- [52] M. A. Ivanov, Y. L. Kalinovsky, and C. D. Roberts, *Phys. Rev. D* **60**, 034018 (1999).
- [53] S. R. Cotanch and P. Maris, *Phys. Rev. D* **66**, 116010 (2002).
- [54] P. Bicudo, *Phys. Rev. C* **67**, 035201 (2003).
- [55] P. Maris (2003), private communication.
- [56] C. H. Llewellyn-Smith, *Ann. Phys.* **53**, 521 (1969).